0026-895X/02/6103-486–494$3.00
MOLECULAR PHARMACOLOGY
Copyright © 2002 The American Society for Pharmacology and Experimental Therapeutics
Mol Pharmacol 61:486–494, 2002

Vol. 61, No. 3
1207/964658
Printed in U.S.A.

Distinct Effects of Different Calcium-Mobilizing Agents on Cell Death in NG108-15 Neuroblastoma X Glioma Cells

TING-YU CHIN, HSIOU-MIN HWANG, and SHEAU-HUEI CHUEH

Department of Biochemistry, National Defense Medical Center, Taipei, Taiwan, Republic of China

Received July 9, 2001; accepted November 19, 2001

This article is available online at http://molpharm.aspetjournals.org

ABSTRACT

The effects of different calcium-mobilizing agents on cell death were characterized in NG108-15 neuroblastoma x glioma hybrid cells. Carbonyl cyanide *p*-trifluoromethoxyphenylhydrazone (FCCP) increased the cytosolic Ca^{2+} concentration ($[Ca^{2+}]_i$) and caused cell death. Thapsigargin (TG) not only increased the $[Ca^{2+}]_i$ and caused cell death but also induced neurite outgrowth via activation of phospholipase A_2 and cytochrome P450 epoxygenase. In contrast, bradykinin increased the $[Ca^{2+}]_i$, but had no effect on cell morphology or cell death. Cell death occurred by two different mechanisms, one of which was caspase-3–dependent and the other caspase-3–independent. Caspase-3 activation was Ca^{2+}-dependent, whereas neurite outgrowth was Ca^{2+}-independent. TG- or FCCP-induced caspase-3 activation occurred at the same time, but the cell death induced by TG was delayed. TG treatment did not enhance the generation of nitric oxide or cAMP or secretion of glial-derived neurotrophic factor or neurotrophin-3, but activated sphingosine kinase. Furthermore, inhibition of sphingosine kinase accelerated TG-induced cell death, and exogenous sphingosine 1-phosphate (S1P) protected cells from FCCP-induced cell death by about 60%. These results indicate that, in these cells, depletion of intracellular nonmitochondrial or mitochondrial Ca^{2+} stores causes cell death, that TG activates phospholipase A_2 and sphingosine kinase, and that arachidonic acid induces neurite outgrowth, whereas S1P delays cell death.

Changes in the cytosolic Ca^{2+} concentration ($[Ca^{2+}]_i$) regulate many cellular functions, including neurotransmission, contraction, secretion, differentiation, cell growth, and cell death (Clapham, 1995; Berridge, 1998). Thus, the process of Ca^{2+} signaling is controlled rapidly and precisely by distinct mechanisms within the cell. Both Ca^{2+} influx and Ca^{2+} release contribute to the Ca^{2+} signal. Ca^{2+} influx is evoked by the activation of voltage-operated Ca^{2+} channels (Hess, 1990) or receptor-operated Ca^{2+} channels (Barnard, 1996) on membrane depolarization or receptor occupancy, respectively, whereas Ca^{2+} release from intracellular Ca^{2+} stores is mediated by the generation of IP_3 (Berridge, 1998) in response to extracellular signals. In addition, Ca^{2+} influx can be activated after depletion of intracellular Ca^{2+} stores via store-operated Ca^{2+} channels (Zhu et al., 1996).

Cells have evolved distinct mechanisms to remove accumulated Ca^{2+} from the cytosol and return the $[Ca^{2+}]_i$ to the resting level after stimulation. The accumulated Ca^{2+} can be either extruded out of the cell via the Ca^{2+} pump and Na^+/Ca^{2+} exchanger in the plasma membrane or sequestered into intracellular Ca^{2+} stores via sarco(endo)plasmic reticulum Ca^{2+} ATPase (SERCA) (Carafoli, 1987; Philipson and Nicoll, 1992). Thus, intracellular Ca^{2+} stores have a dual role; they can release Ca^{2+} to generate the Ca^{2+} signal during stimulation and can accumulate Ca^{2+} to buffer Ca^{2+} in the resting state. There is evidence that mitochondria also play an important role in Ca^{2+} signaling. Ca^{2+} undergoes continuous cyclic movement across the mitochondrial inner membrane, the mitochondrial uniporter using an internally negative membrane potential to accumulate Ca^{2+}, whereas Na^+-independent efflux is driven by the pH gradient and Na^+-dependent efflux exchanges Ca^{2+} for Na^+ (Denton and McCormack, 1990; Gunter et al., 1994).

Using neuroblastoma x glioma NG108-15 cells, we have previously shown that the bradykinin (BK)-induced $[Ca^{2+}]_i$ increase is predominantly attributable to IP_3-evoked intracellular Ca^{2+} release. Furthermore, thapsigargin (TG), the SERCA inhibitor, and carbonyl cyanide *p*-trifluoromethoxyphenylhydrazone (FCCP), the protonophore, blocked Ca^{2+} loading into endoplasmic reticulum and mitochondria by inhibiting SERCA and destroying the mitochondrial membrane potential, respectively. After TG or FCCP treatment, an increased $[Ca^{2+}]_i$ was seen because of the discharge of entrapped Ca^{2+} from respective organelles and Ca^{2+} content

This work was supported by grants from the National Science Council (NSC89-2320-B016-096) and the National Defense Medical Center (DOD-90-33), Republic of China.

ABBREVIATIONS: SERCA, sarco(endo)plasmic reticulum Ca^{2+} ATPase; BK, bradykinin; TG, thapsigargin; FCCP, carbonyl cyanide *p*-trifluoromethoxyphenylhydrazone; FDA, fluorescein diacetate; PI, propidium iodide; $AACOCF_3$, arachidonyl trifluoromethyl ketone; HELSS, bromoenol lactone; GDNF, glial-derived neurotrophic factor, NT-3, neurotrophin-3; S1P, sphingosine 1-phosphate.

within these two organelles was depleted. Thus, BK, TG, and FCCP all evoked $[Ca^{2+}]_i$ increase, but the underlying mechanisms are distinct (Chueh and Kao, 1994; Chueh et al., 1995; Hsu et al., 1995). It is believed that a prolonged $[Ca^{2+}]_i$ increase promotes cell death. In nerve cells, glutamate-induced cell death, so called excitotoxicity, is attributed to a $[Ca^{2+}]_i$ increase (Choi, 1988). Evidence also suggests that intraluminal Ca^{2+} within endoplasmic reticulum or matrix Ca^{2+} within mitochondria is linked to control of cell growth and cell death (Short et al., 1993; Ichas and Mazat, 1998; Paschen and Doutheil, 1999). To discriminate whether the depletion of intraluminal Ca^{2+} or matrix Ca^{2+}, or the sustained $[Ca^{2+}]_i$ increase is critical for cell death, in this study, using NG108-15 cells, we compared the effect of BK, TG and FCCP on cell death. Although all three agents induced a transient $[Ca^{2+}]_i$ increase, only TG and FCCP caused cell death. TG-induced cell death was delayed by the generation of sphingosine 1-phosphate. TG also induced neurite outgrowth via the generation of arachidonic acid.

Materials and Methods

Cell Culture. Neuroblastoma x glioma hybrid NG108-15 cells were cultured as described previously (Chueh et al., 1995). In brief, cells (passage 22–40) were cultured in Dulbecco's modified Eagle's medium supplemented with 5% fetal bovine serum, 100 μM hypoxanthine, 1 μM aminopterin, and 16 μM thymidine (Invitrogen, Carlsbad, CA), and were maintained at 37°C in an atmosphere of 95% air and 5% CO_2. All experiments were performed using nondifferentiated cells.

Neurite Outgrowth Assay. Cells were grown in six-well plates and reached 50 to 70% confluence. After cells have been treated with buffer or 1 μM TG with or without the indicated drugs for 3 h, neurite outgrowth was assessed. Processes longer than twice the diameter of the cell body were scored as neurites. Neurite-positive cells were quantified in 10 randomly chosen fields, about 50 to 70 cells in each field, from each well, and the percentage of cells with neurites was calculated. The experiments were repeated 8 to 11 times using different batches of cells. One representative morphology of cells from each experiment is illustrated in Fig. 3, and the mean ± S.E.M. values for the percentage of cells with neurites, calculated for n experiments using different batches of cells, are shown in Fig. 4.

Measurement of the $[Ca^{2+}]_i$. The $[Ca^{2+}]_i$ change in a single cell, grown on coverslips, was measured using the fluorescent Ca^{2+} indicator, fura-2 (Molecular Probes, Eugene, OR), in loading buffer (150 mM NaCl, 5 mM KCl, 5 mM glucose, 1 mM $MgCl_2$, 2.2 mM $CaCl_2$, and 10 mM HEPES, pH 7.4) as described previously (Chin and Chueh, 1998). The $[Ca^{2+}]_i$ was calculated from the ratio of the fluorescence at 340 nm and 380 nm according to the equation derived by Grynkiewicz et al. (1985) using parameters obtained on our instrument (Spex Industries, Edison, NJ) for fura-2 in NG108-15 cells: R_{min}, 0.66; R_{max}, 2.6; S_{f2}/S_{b2}, 2.43; and K_d, 135 nM. The results of one representative experiment are illustrated in the figures, and the mean ± S.D. values for the $[Ca^{2+}]_i$ changes, calculated for n experiments using different batches of cells, are given in the text.

Caspase-3 Assay. Caspase-3 activity was measured using a caspase-3 assay kit (BD PharMingen, San Diego, CA) according to the manufacturer's instructions. Briefly, after exposure to the drugs, cells grown in 60 mm dishes were detached and lysed with 500 μl of lysis buffer (10 mM Tris-HCl, 10 mM NaH_2PO_4/Na_2HPO_4, 130 mM NaCl, 1% Triton X-100, and 10 mM sodium pyrophosphate, pH 7.4). Aliquots (50 μl) of lysate were mixed with 10 μl of DEVD-7-amino-4-methylcoumarin (1 μg/μl; a fluorogenic caspase-3 substrate) and 1 ml of HEPES buffer (20 mM HEPES, 10% glycerol, and 2 mM dithiothreitol, pH 7.5), incubated for 60 min at 37°C, and the fluorescence of the liberated product measured using a spectrofluorometer (Spex). The emission fluorescence spectrum was scanned between 400 nm and 500 nm using an excitation wavelength of 380 nm, caspase-3 activity giving a maximum at 440 nm. Experiments were repeated six times using different batches of cells with similar results.

Determination of Cyclic AMP Generation. Briefly, after near-confluence was reached in six-well plates, the cells were incubated with various drugs for the indicated time in 1 ml of loading buffer, then the amount of cyclic AMP generation by the cells in each well was determined using a [^{3}H]cyclic AMP assay system (Amersham Biosciences, Little Chalfont, Buckinghamshire, UK), according to the manufacturer's instructions, as described previously (Chueh et al., 1995). The same experiments were carried out four times in triplicate using different batches of cells. The data are presented as mean ± S.E.M.

Assay of Arachidonic Acid Release. Arachidonic acid release from NG108-15 cells was measured as described previously (Chen et al., 1998). Briefly, cells grown in 24-well plates were loaded with [^{3}H]arachidonic acid by addition of 330 nCi/ml of [^{3}H]arachidonic acid in 200 μl of loading buffer to each well and incubation at 37°C for 15 h. After unincorporated [^{3}H]arachidonic acid was removed by thorough washing, the cells were stimulated for 5 min with various test agents in loading buffer. The radioactivity accumulated in the buffer (supernatant, S) or cells (pellet, P) was measured, and [^{3}H]arachidonic acid release expressed as a percentage of the total incorporated [^{3}H]arachidonic acid, calculated as $S / (P + S) \times 100$. Experiments were repeated six times in triplicate, using different batches of cells. The data are presented as mean ± S.E.M.

Determination of Nitric Oxide Concentration. NO in the medium was measured as its stable metabolite, nitrite, as described previously (Bi and Reiss, 1995). Briefly, after incubation of the cells in six-well plates in loading buffer in the presence or absence of various drugs, 100-μl aliquots of medium were mixed with an equal volume of Greiss reagent (1% sulfanilamide, 0.1% N-1-naphthylethylenediamine, and 5% H_3PO_4) and the absorbance at 540 nm measured after incubation at 37°C for 15 min. Serial dilutions of a known stock solution of sodium nitrite were used to generate a standard curve for each measurement. The experiments were repeated six times, in triplicate, using different batches of cells. The data presented are the mean ± S.E.M.

Assessment of Cell Viability. The viability of NG108-15 cells was evaluated by double-staining with fluorescein diacetate (FDA) and propidium iodide (PI) as described previously (Jones and Senft, 1985). After the indicated treatment, the cells, grown on coverslips, were incubated for 5 min at room temperature with 10 μg/ml of FDA and 3 μg/ml of PI in loading buffer, then washed with the same buffer. FDA-stained viable cells and PI-stained nonviable cells emit green and red fluorescence, respectively. Both types of fluorescent cells were viewed using a standard fluorescence microscope (Axiophot; Zeiss, Jena, Germany). Experiments were repeated six times using different batches of cells with similar results. The results of one representative experiment are illustrated.

Measurement of Sphingosine Kinase Activity. Sphingosine kinase activity in the cells was measured by minor modifications of a method described previously (Edsall et al., 1997). After exposure to drugs, cells grown in 10-cm dishes were detached, suspended in 200 μl of buffer A [50 mM Tris-HCl, pH 7.4, 20% (v/v) glycerol, 1 mM mercaptoethanol, 1 mM EDTA, 1 mM Na_3VO_4, 15 mM NaF, 10 μg/ml of leupeptin, 10 μg/ml of aprotinin, 1 mM phenylmethylsulfonyl fluoride, and 0.5 mM 4-deoxypyridoxine], lysed by freeze-thawing three times, and centrifuged at 13,000g for 30 min. Aliquots (50 μl) of supernatant (approximately 50 μg of protein) were mixed with 5 μl of 400 μM sphingosine, 10 μl of 20 mM [γ-^{32}P]ATP (20 μCi), 10 μl of 10 mg/ml bovine serum albumin, 5 μl of 200 mM $MgCl_2$, and 120 μl of buffer A, and incubated for 30 min at 37°C. The reaction was terminated by adding 20 μl of 1 N HCl, then lipids were extracted using 0.8 ml of chloroform/methanol/concentrated HCl [100:200:1

(v/v)]. After vigorous vortexing, 240 μl of chloroform and 240 μl of 2 M KCl were added for phase separation. The lipids in the organic phase and unlabeled authentic sphingosine 1-phosphate were spotted onto silica gel 60 thin-layer chromatography plates and chromatographed using 1-butanol/methanol/acetic acid/water [80:20:10:20 (v/v)] as the solvent system. The radioactive spots were visualized by autoradiography and the authentic sphingosine 1-phosphate spot by spraying with ninhydrin.

Secretion of GDNF and NT-3. The amount of GDNF or NT-3 secreted by the cells was determined using an immunoassay system (Promega, Madison, WI) according to the manufacturer's instructions. Briefly, after near-confluence was reached in six-well plates, the cells were incubated with various drugs for the indicated time in 1 ml of loading buffer, then the reaction was terminated by addition of 100 μl of 1 N HCl. After the cells were scraped off the plates and centrifuged at 13,000*g* for 15 min, the supernatant was neutralized and an aliquot used to determine the amount of GDNF and NT-3. The same experiments were carried out four times in triplicate using different batches of cells. The data presented are the mean ± S.E.M.

Determination of Nuclear Changes. The chromatin-specific dye Hoechst 33258 was used to observe nuclear changes occurring during the process of cell death. After the indicated treatments, cultured cells, grown on coverslips, were fixed for 10 min at room temperature with 3% paraformaldehyde and washed twice with phosphate-buffered saline. They were then stained for 20 min at room temperature with 10 μM Hoechst 33258 (Sigma) in phosphate-buffered saline. Nuclear morphology was examined on an Olympus IX-70 fluorescence microscope with excitation and emission wavelengths of 350 and 460 nm, respectively. The nuclei of control cells appeared oval, whereas apoptotic nuclei were identified by chromatin condensation or clumping. Apoptotic and nonapoptotic nuclei were counted in 10 randomly chosen fields per coverslip. The percentage of apoptotic cells was expressed as the mean ± S.E.M. for *n* experiments.

Results

Fig. 1 shows the effect of three different Ca^{2+}-mobilizing agents, FCCP, TG, and BK, (all at 1 μM) on the $[Ca^{2+}]_i$ and morphology of NG108-15 cells. Results in the presence of extracellular Ca^{2+} are shown in Fig. 1A, traces a–c. FCCP, a lipophilic protonophore that blocks mitochondrial Ca^{2+} accumulation by dissipating the internal negative mitochondrial potential, should induce loss of sequestered Ca^{2+} from the mitochondria. In NG108-15 cells, a rapid $[Ca^{2+}]_i$ increase was indeed induced by FCCP, and the $[Ca^{2+}]_i$ remained at a sustained level for 150 s after FCCP addition (Fig. 1A, trace a). A slower and lower $[Ca^{2+}]_i$ increase was evoked when cells were treated with TG, a SERCA inhibitor (Fig. 1A, trace b). BK, a phospholipase C-coupled hormone, also induced a rapid $[Ca^{2+}]_i$ increase, followed by a decline to the basal level (Fig. 1A, trace c). In the presence of extracellular Ca^{2+}, the $[Ca^{2+}]_i$ increase induced by FCCP, TG, and BK was 430 ± 39 nM, 141 ± 28 nM, and 375 ± 45 nM (n = 22), respectively. In the absence of extracellular Ca^{2+}, a similar $[Ca^{2+}]_i$ increase was seen with TG or BK (Fig. 1B, traces e and f), whereas the FCCP-induced $[Ca^{2+}]_i$ increase was profoundly inhibited (Fig. 1B, trace d). Although all these three compounds induced a $[Ca^{2+}]_i$ increase in NG108-15 cells in the presence of extracellular Ca^{2+}, they had distinct effect on cellular morphology. As shown in Fig. 1B, compared with control cells, the morphology of the cells was unchanged after 3-h treatment with BK. However, after FCCP treatment, the cells became smaller and unhealthy, whereas, after TG treatment, more processes were formed and the cell bodies rounded up, a typical morphology of the differentiated NG108-15 cells induced by cyclic AMP (Nirenberg et al., 1983). Other SERCA inhibitors, including 2,5-di-*tert*-butylhydroquinone and cyclopiazonic acid, had an effect similar to that of TG on the morphology of NG108-15 cells (data not shown).

To elucidate the molecular mechanism underlying the morphological changes, we measured arachidonic acid release, NO production, and cAMP generation after exposure of the cells to FCCP, TG, or BK. As shown in Fig. 2A, only TG induced arachidonic acid release; the amount released after 2 h exposure was about 8-fold greater than the basal level. None of the three agents resulted in NO or cAMP generation (Fig. 2, B and C).

We next determined whether the neurite outgrowth observed in TG-treated cells was mediated by the release of arachidonic acid. If this were the case, a similar morphology would be expected when exogenous arachidonic acid was added to the culture medium. We examined the effect on neurite outgrowth of five different 20-carbon fatty acids with 0, 1, 2, 3, or 4 double bonds. As shown in Fig. 3, c–g, *cis*-5,8,11,14-eicosatetraenoic acid (arachidonic acid) (20:4) had a similar effect to TG on neurite outgrowth, *cis*-8,11,14-eicosa-

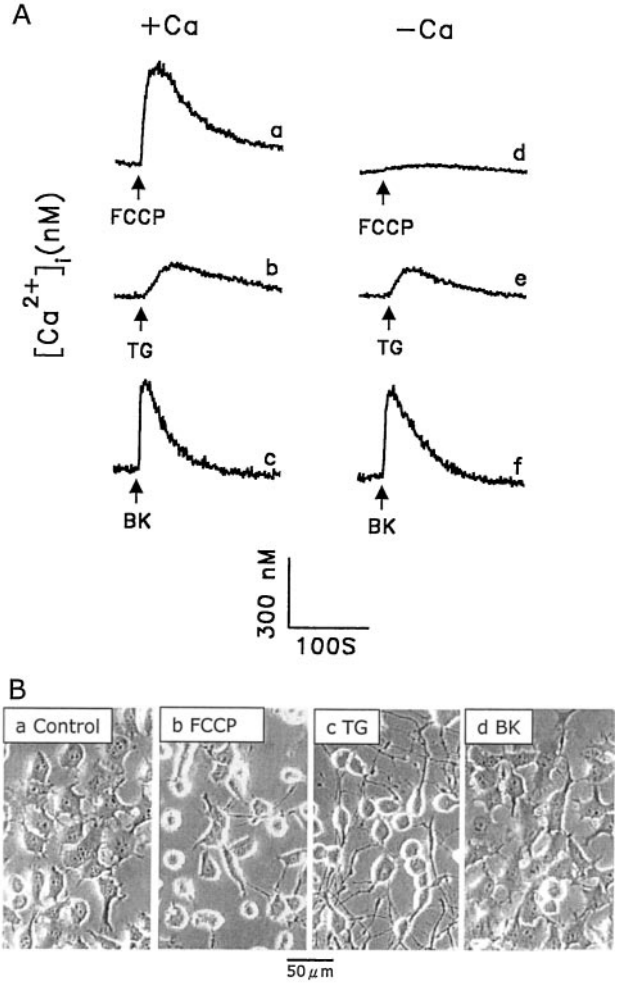

Fig. 1. Effects of FCCP, TG, and BK on the $[Ca^{2+}]_i$ and morphological changes in NG108-15 cells. A, the $[Ca^{2+}]_i$ change was measured in a single cell in response to addition of 1 μM FCCP (traces a and d), 1 μM TG (traces b and e), or 1 μM BK (traces c and f) in the presence (a–c) or absence (d–f) of extracellular Ca^{2+}. B, cellular morphology. Cells were treated for 3 h with the indicated drug at the same concentration as in A.

trienoic acid (20:3) had a partial effect, and *cis*-11,14-eicosadienoic acid (20:2), *cis*-11-eicosenoic acid (20:1), and *n*-eicosanoic acid (20:0) had no effect. The percentage of neurite positive cells after treatment with TG or five different 20-carbon fatty acids with zero, one, two, three, or four double bonds, respectively, is 87.0 ± 5.4, 14.8 ± 4.8, 13.3 ± 3.7, 17.8 ± 3.1, 43.1 ± 5.4, and 72.2 ± 6.4% (n = 10). The results shown in Fig. 2 already suggested that NO and cAMP were not involved in the TG-induced morphology changes, and this was confirmed by the lack of effect of N^G-monomethyl-L-arginine (an NO synthase inhibitor) or SQ22536 (an adenylyl cyclase inhibitor) on TG-induced neurite outgrowth (Fig. 3, h and i); the corresponding percentages of cells with neurite were 83.1 ± 2.1 and 85.8 ± 2.2% (n = 10), respectively. Similarly, the percentage of cells with neurite induced by TG in the presence of DEVD-CHO (a capase-3 inhibitor), staurosporine (a broad-specificity protein kinase inhibitor), or BAPTA/AM (a Ca^{2+} chelator) was not significantly different from that induced by TG alone: 82.5 ± 3.2, 83.7 ± 4.5, and 87.2 ± 1.4 (n = 10), respectively, (Fig. 3, j–l), whereas the phospholipase A_2 inhibitors $AACOCF_3$ and HELSS caused significant inhibition on TG-induced neurite outgrowth (Fig. 3, m and n); the percentages of cells with neurite were 51.7 ± 3.2% ($p < 0.001$) and 58.1 ± 4.6% (n = 11) ($p < 0.001$), respectively, further confirming that neurite outgrowth was mediated by arachidonic acid release. The IC_{50} values for $AACOCF_3$ and HELSS are 2.5 μM and 0.8 μM, respectively (data not shown). It is possible that the morphological change induced by TG is mediated by downstream metabolites of arachidonic acid. As shown in Fig. 3, o-q, TG-induced neurite outgrowth was unaffected by the cyclooxygenase inhibitor ebselen and the lipoxygenase inhibitor nordihydroguaiaretic acid, but significantly inhibited by the cytochrome P450 epoxygenase inhibitor SKF525A; the percentage of neurite-positive cells was 81.1 ± 8.1, 86.6 ± 3.7, and 52.2 ± 6.7 ($p < 0.001$) (n = 9), respectively. Figure 4 summarizes the statistical data measured in Fig. 3.

We next determined whether these three Ca^{2+}-mobilizing agents caused cell death in NG108-15 cells, by measuring the

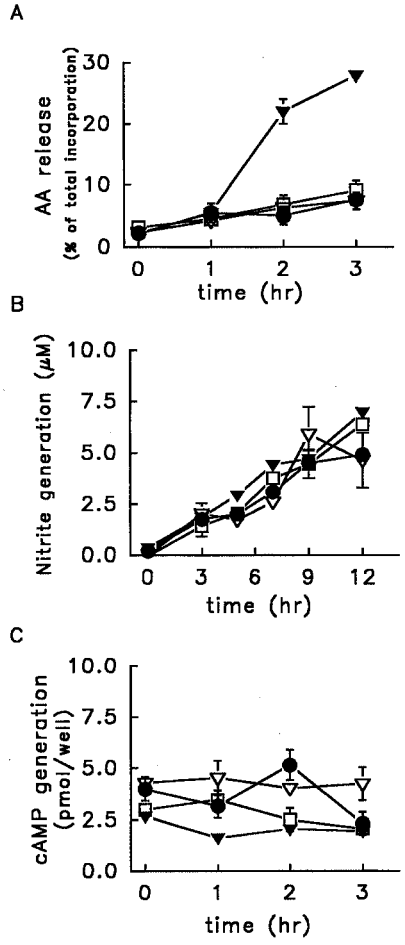

Fig. 2. Effects of FCCP, TG, and BK on arachidonic acid release, nitrite generation, and cAMP formation in NG108-15 cells. A, prelabeled NG108-15 cells were stimulated with buffer (●), 1 μM FCCP (▽), 1 μM TG (▼), or 1 μM BK (□), and the release of radioactivity into the medium was assayed at different time-points. The results are expressed as the percentage of the total radioactivity incorporated into the cells. B, NO generated in the extracellular solution was measured as its end product, nitrite, after the cells were treated with buffer (●), 1 μM FCCP (▽), 1 μM TG (▼), or 1 μM BK (□) for the indicated time. C, intracellular cyclic AMP accumulation was measured after treatment of the cells with buffer (●), 1 μM FCCP (▽), 1 μM TG (▼), or 1 μM BK (□) for the indicated time. The data are the mean ± S.E.M. of four to six independent experiments.

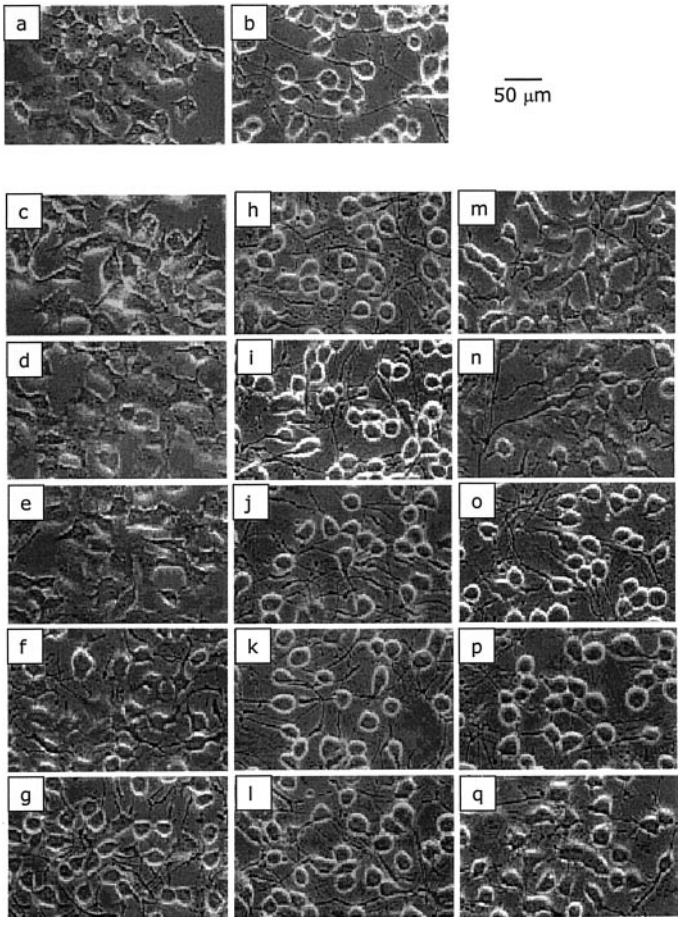

Fig. 3. Effects of different 20-C fatty acids on neurite outgrowth and of various inhibitors on TG-induced morphological changes in NG108-15 cells. All pictures were taken after 3 h of drug exposure. The cellular morphology after treatment with buffer (a) or 1 μM TG (b) is shown for comparison. Cells were treated with 10 μM *n*-eicosanoic acid (c), *cis*-11-eicosenoic acid (d), *cis*-11,14-eicosadienoic acid (e), *cis*-8,11,14-eicosatrienoic acid (f), or *cis*-5,8,11,14-eicosatetraenoic acid (g). Cells were also treated with 1 μM TG in the presence of 100 μM N^G-monomethyl-L-arginine (h), 10 μM SQ22536 (i), 10 μM DEVD-CHO (j), 0.3 μM staurosporine (k), 3 μM BAPTA/AM (l), 3 μM $AACOCF_3$ (m), 10 μM HELSS (n), 5 μM ebselen (o), 5 μM nordihydroguaiaretic acid (p), or 30 μM SKF525A (q).

integrity of plasma membrane and nuclear changes as indicators of cell death. First, we measured caspase-3 activity after cells have been treated with buffer, FCCP, TG, or BK for the indicated time. As shown in Fig. 5A, in the presence of extracellular Ca^{2+}, caspase-3 activity, indicated, by the fluorescence intensity emitted at 440 nm, increased at 3 h after treatment of cells with FCCP or TG; it then gradually declined to the basal level in FCCP-treated cells, but continued to increase and peaked between 5 and 7 h in TG-treated cells. In contrast, BK did not induce caspase-3 activation. In the absence of extracellular Ca^{2+}, FCCP-induced caspase-3 activation was abolished, whereas TG-induced caspase-3 activation was unaffected. Figure 5B shows the time course of cell death determined by chromatin condensation and clumping after exposure to drugs in the presence or absence of extracellular Ca^{2+}. In the presence of extracellular Ca^{2+}, FCCP-induced caspase-3 activation coincided with cell death, whereas, in the absence of extracellular Ca^{2+}, significant cell death was still induced by FCCP at 3 h, but caspase-3 activity was low. However, TG-induced caspase-3 activation did not coincide with cell death, which was not seen until 7 h in both the presence and absence of extracellular Ca^{2+}, indicating that cell death induced by TG was delayed. In addition, inhibition of caspase-3 activity by 10 μM DEVD-CHO significantly blocked TG-induced cell death; the percentage of apoptotic cells induced by TG decreased from 46 ± 8% to 19 ± 6% (n = 6) 7 h after TG treatment in the absence of extracellular Ca^{2+} (data not shown). About 75% of cells were apoptotic after 9 h exposure to FCCP or TG in both the presence and absence of extracellular Ca^{2+}. BK did not induce cell death. Similar results were seen when cell death was measured by PI uptake (Fig. 6). After 3-h treatment with FCCP, 34% of cells took up PI, and this increased to 66 and 92% after 5 and 7 h, respectively. However, TG-induced PI uptake was delayed until 7 h. Again, no PI uptake was seen in cells exposed to BK for at least 9 h, indicating that the cells were viable.

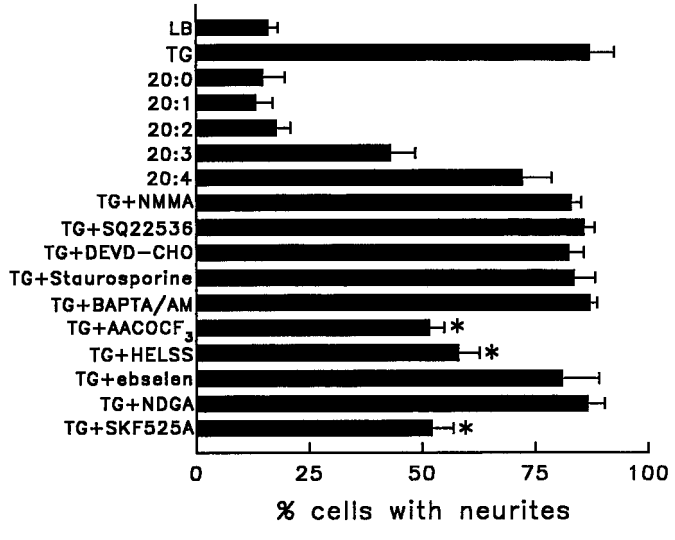

Fig. 4. Quantitative analysis of neurite outgrowth measured in Fig. 3. Percentage of neurite-bearing cells were quantified in each condition described in Fig. 3, a to q. The data are the mean ± S.E.M. values for the percentage of cells with neurite, calculated for 9 to 11 experiments using different batches of cells. *, $p < 0.001$; significant decrease in neurite-bearing cells after $AACOCF_3$, HELSS, and SKF525A treatment.

These results indicated that the activity of caspase-3 increased at 3 h after treatment of cells with both FCCP and TG but that in TG-treated cells, death was delayed. TG might also induce the generation of a protective factor that slows cell death. We next examined whether TG induced the generation of GDNF or NT-3. As shown in Fig. 7, none of the three test agents caused increased generation of GDNF (Fig.

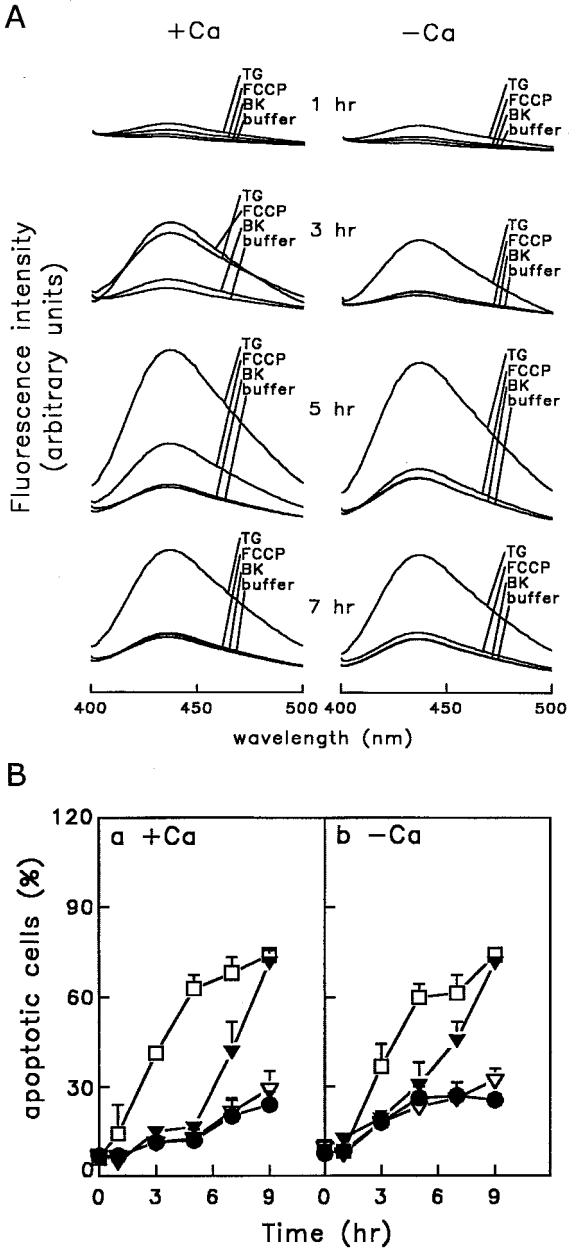

Fig. 5. Effects of FCCP, TG, and BK on caspase-3 activation and apoptotic cell death in the presence or absence of extracellular Ca^{2+}. A, the emission fluorescence spectra (400–500 nm) of the cleavage product of caspase-3 after treatment of NG108-15 cells with buffer, 1 μM FCCP, 1 μM TG, or 1 μM BK for the indicated time in the presence (left traces) or absence (right traces) of extracellular Ca^{2+} are shown. Experiments were repeated six times with similar results; one representative trace is shown. B, after cells were treated with buffer (●), 1 μM FCCP (□), 1 μM TG (▼), or 1 μM BK (▽) for the indicated time in the presence (a) or absence (b) of extracellular Ca^{2+}, the number of apoptotic cells was determined by chromatin condensation or clumping and expressed as a percentage of the total cells in the field. Data are the mean ± S.E.M. of four independent experiments using different batches of cells.

7A) or NT-3 (Fig. 7B). We then examined whether the increased generation of arachidonic acid induced by TG might play a role in slowing the process of cell death. If this were the case, exogenously added arachidonic acid would be expected to have a similar protective effect on FCCP-induced cell death. As shown in Fig. 7C, 1 μM arachidonic acid itself did not cause cell death or protect cells from FCCP-induced cell death; approximately 50% of the cells were apoptotic after 3-h treatment with FCCP, regardless of the presence or absence of arachidonic acid. In contrast, sphingosine 1-phosphate (S1P), which protects Jurkat T lymphocytes from Fas- and ceramide-mediated apoptosis (Cuvillier et al., 1996), had a significant protective effect against FCCP-induced cell death; the percentage of apoptotic cells measured after 3 h of FCCP treatment decreasing from about 50 to 27% in the presence of 10 μM S1P.

We next tested whether S1P could retard the process of FCCP-induced cell death. As shown in Fig. 8A, a, in the absence of S1P, chromatin condensation and clumping did not occur until 7 h after exposure to TG but were seen as early as 3 h after exposure to FCCP, consistent with the results shown in Fig. 5. In the presence of 1 μM S1P, FCCP-induced chromatin condensation and clumping were reduced; the percentage of apoptotic cells was 22 and 30% after 3- and 5-h exposure to FCCP (Fig. 8A, b). The corresponding values in the absence of S1P were 36 and 60%, respectively (Fig. 8A,

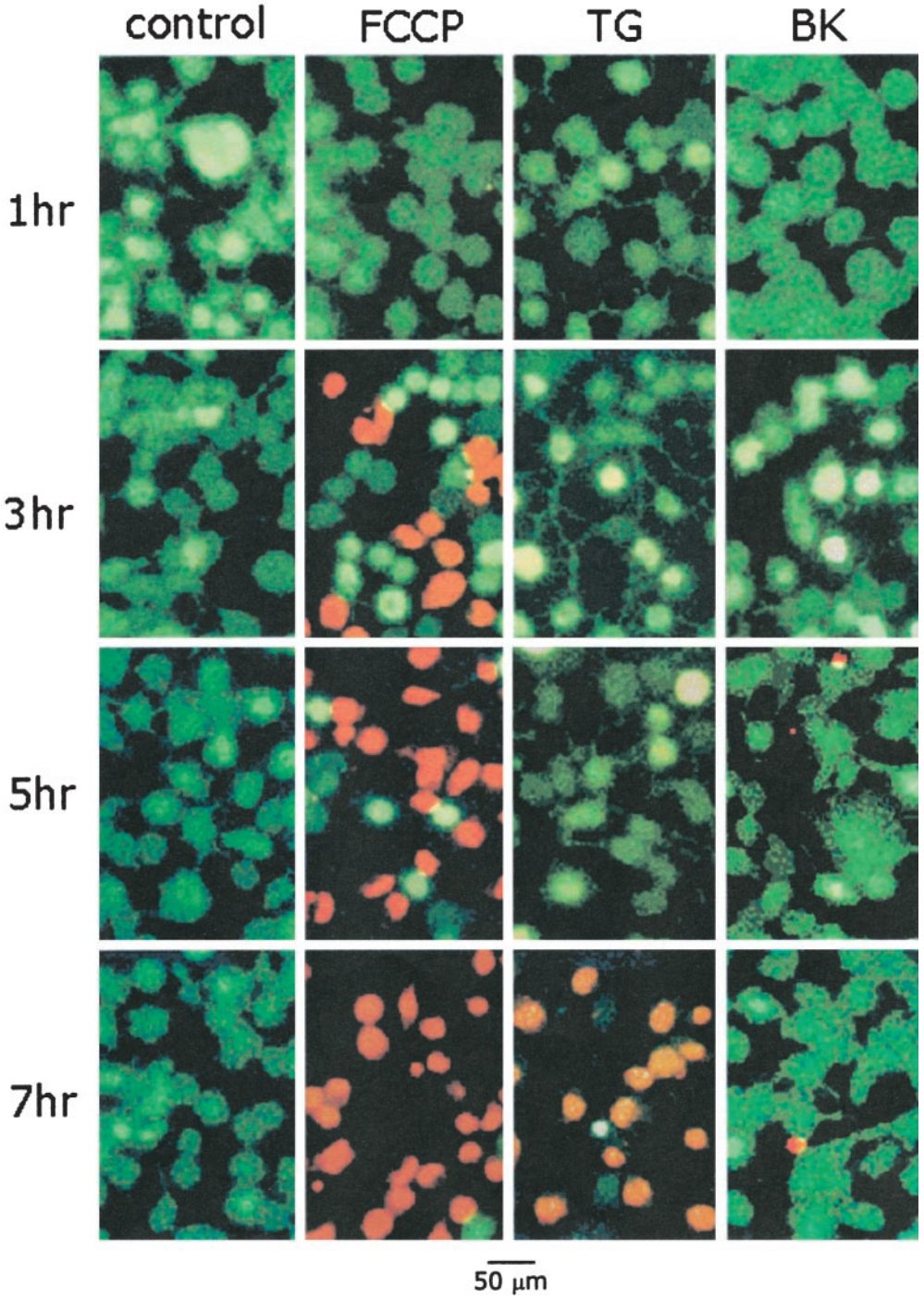

Fig. 6. Effects of FCCP, TG, and BK on cell death. Cells were treated with buffer, 1 μM FCCP, 1 μM TG, or 1 μM BK for the indicated time, then double-stained with FDA and PI for 5 min before being photographed using a fluorescence microscope. Green fluorescence represents living cells, whereas red fluorescence represents dead cells. The results shown are from a representative field of a typical experiment performed six times with similar results.

a). These results indicated that the delay in cell death seen with TG treatment compared with FCCP treatment might be caused by S1P generation. If this were the case, then synchronized caspase-3 activation and cell death would be expected if S1P generation were prevented by inhibition of sphingosine kinase. We therefore examined cell death induced by FCCP, TG, and BK in the presence of the sphingosine kinase inhibitor, *N*,*N*-dimethylsphingosine. As shown in Fig. 8A, c, cell death induced by FCCP or TG was accelerated in the presence of *N*,*N*-dimethylsphingosine; TG-induced cell death was indistinguishable from that induced by FCCP for up to 5 h after drug exposure. We finally measured sphingosine kinase activity in NG108-15 cells treated with FCCP, TG, and BK. As shown in Fig. 8B, after 3-h exposure to drugs, sphingosine kinase activity in TG-treated cells was higher than in control cells, whereas the activity in FCCP-treated cells was lower than in controls. Sphingosine kinase activity in BK-treated cells was indistinguishable from that in control cells. Inhibition of phospholipase A_2 by $AACOCF_3$ did not result in any change in sphingosine kinase activity induced by FCCP, TG, or BK (data not shown).

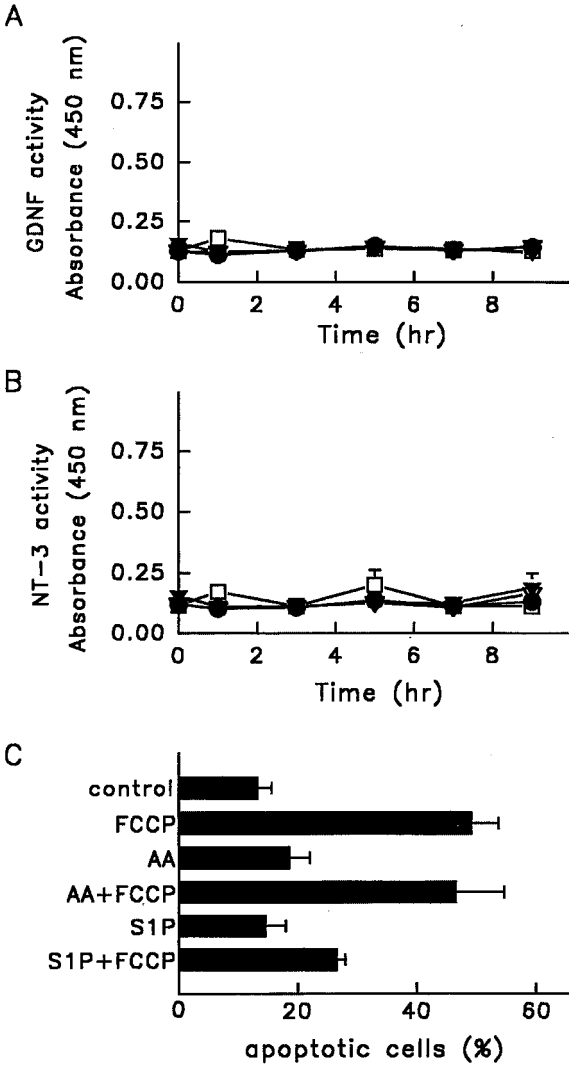

Fig. 7. Effects of FCCP, TG, and BK on the generation of GDNF and NT-3, and protective effect of S1P on FCCP-induced cell death. The concentration of GDNF (A) and NT-3 (B) in the extracellular solution were measured after cells were treated with buffer (○), 1 μM FCCP (▽), 1 μM TG (▼), or 1 μM BK (□) for the indicated time. C, cells were treated with buffer (control), 1 μM FCCP (FCCP), 1 μM arachidonic acid (AA), 1 μM arachidonic acid + 1 μM FCCP (AA + FCCP), 10 μM S1P (S1P), or 10 μM S1P + 1 μM FCCP (S1P + FCCP) and the apoptotic cells counted after 3 h and expressed as a percentage of the total cells. The data are the mean ± S.E.M. of four independent experiments using different batches of cells.

Discussion

In an attempt to characterize the correlation among the increase of $[Ca^{2+}]_i$, the depletion of intracellular Ca^{2+} stores and cell death, the effects of three different Ca^{2+}-mobilizing agents on cell death were measured. Our results show that TG, BK, and FCCP all evoked an increase in the $[Ca^{2+}]_i$ in NG108-15 cells; however, only FCCP and TG caused cell death. TG prevents the uptake of Ca^{2+} into Ca^{2+} stores by inhibiting the SERCA and gradually leads to Ca^{2+} depletion via leak channels. Although BK stimulates Ca^{2+} release from intracellular Ca^{2+} stores via the generation of IP_3, it is possible that intraluminal Ca^{2+} levels were not depleted because the Ca^{2+} stores can be refilled by Ca^{2+} uptake via the

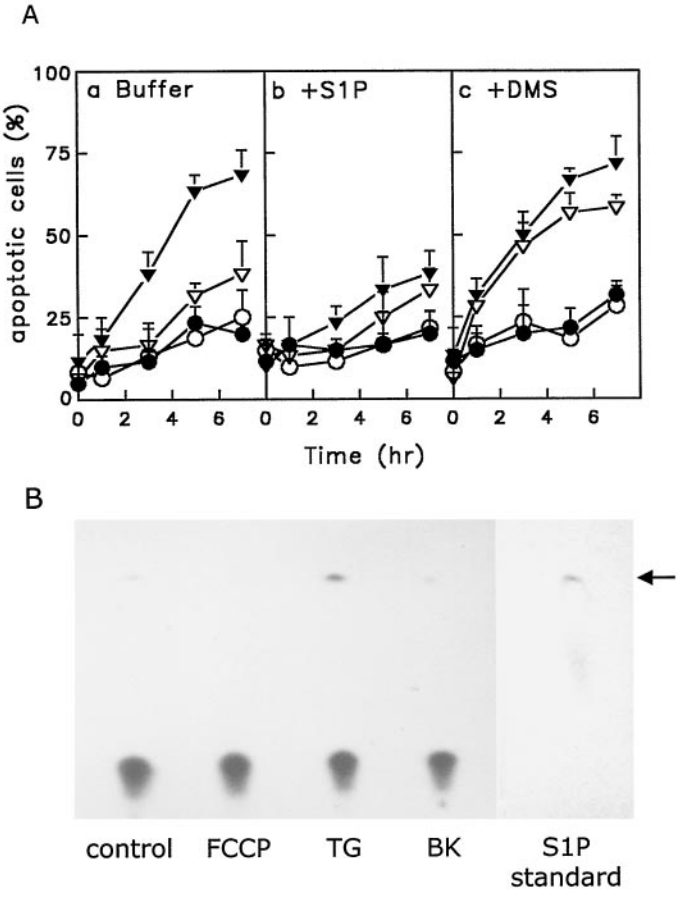

Fig. 8. Effect of S1P and *N*,*N*-dimethylsphingosine on cell death, and the effects of FCCP, TG, and BK on sphingosine kinase activity. A, apoptotic cell death was measured after cells were treated with buffer (○), 1 μM FCCP (▼), 1 μM TG (▽), or 1 μM BK (●) for the indicated time in the absence (a) or presence (b) of 10 μM S1P or the presence (c) of 10 μM *N*,*N*-dimethylsphingosine (DMS). The data are the mean ± S.E.M. of four independent experiments using different batches of cells. B, autoradiogram of the thin-layer chromatography plate demonstrating increased and reduced formation of S1P (indicated by the arrow) after 3-h treatment of cells with 1 μM TG and 1 μM FCCP, respectively. The right lane is the authentic S1P standard visualized by ninhydrin. Experiments were repeated five times with similar results.

SERCA (Chueh and Kao, 1994; Chueh et al., 1995). Disruption of the mitochondrial membrane potential by the protonophore FCCP not only inhibits Ca^{2+} accumulation within mitochondria, but also causes the release of trapped Ca^{2+} from the mitochondria (Huang and Chueh, 1996). Taken together, our results suggest that depletion of intracellular nonmitochondrial or mitochondrial Ca^{2+} stores, rather than a transient increase in the $[Ca^{2+}]_i$, induces cell death. Similarly, in human prostatic carcinoma LNCaP cells, intracellular Ca^{2+} store depletion triggers apoptosis without a requirement for a sustained $[Ca^{2+}]_i$ increase (Wertz and Dixit, 2000; Skryma et al., 2000).

Presumably, the increased $[Ca^{2+}]_i$ induced by TG, BK, and FCCP all originated from the intracellular Ca^{2+} stores, endoplasmic reticulum, or mitochondria, and should be independent to the extracellular Ca^{2+}. To our surprise, in the absence of extracellular Ca^{2+}, FCCP-induced $[Ca^{2+}]_i$ increase was not seen (Fig. 1A). These data indicate that, in NG108-15 cells, the $[Ca^{2+}]_i$ influx might be induced by mitochondrial Ca^{2+} depletion. Recently, Gonzalez et al. (2000) have shown that, in mouse pancreatic acinar cells, Ca^{2+} release from mitochondria can only be induced by FCCP after prior agonist exposure, because Ca^{2+} accumulates within the matrix after agonist exposure, whereas the mitochondria contain no releasable Ca^{2+} under resting conditions. However, a $[Ca^{2+}]_i$ increase was still evoked by FCCP under resting conditions in the absence of a drop in the mitochondrial Ca^{2+} concentration, indicating that the Ca^{2+}, mobilized by FCCP, originates from a compartment other than the mitochondria. This result supports our finding in the current study. Alternatively, it is possible that the Ca^{2+} concentration within the matrix might be tightly linked to extracellular Ca^{2+} levels in NG108-15 cells. Once extracellular Ca^{2+} is removed, the matrix Ca^{2+} leaks rapidly and no more Ca^{2+} would be released, even though the membrane potential was destroyed.

The TG-induced $[Ca^{2+}]_i$ increase and caspase-3 activation were not affected by removal of extracellular Ca^{2+} (Figs. 1A and 5A), whereas, in the absence of extracellular Ca^{2+}, the FCCP-induced $[Ca^{2+}]_i$ increase was significantly reduced by approximately 95% (Fig. 1A), as was FCCP-induced caspase-3 activation (Fig. 5A). These results suggest that caspase-3 activation in NG108-15 cells is Ca^{2+}-dependent. The fact that FCCP-induced cell death was still seen in the absence of extracellular Ca^{2+} (Fig. 4B) suggests that death was mediated by a caspase-3 independent pathway which is Ca^{2+}-insensitive. It could be possible that FCCP- and TG-induced cell death both are mediated by caspase-3 independent pathway, because TG-induced caspase-3 activation did not coincide with cell death. TG failed to induce cell death after caspase-3 was inhibited, suggesting the dependence of cell death on caspase-3. Thus, two mechanisms lead to cell death in NG108-15 cells, one caspase-3–dependent, the other caspase-3–independent.

Previously, using a rat cerebellum membrane preparation, we showed that mitochondria are 10 times more sensitive than microsomes in terms of the arachidonic acid-induced release of accumulated Ca^{2+}. Similarly, in permeabilized NG108-15 cells, mitochondria still exhibit a higher organelle-specific sensitivity to the arachidonic acid-induced release of accumulated Ca^{2+} (Huang and Chueh, 1996). In the current study, TG activated phospholipase A_2 to generate significant arachidonic acid release. It is possible that part of the TG-induced increase in the $[Ca^{2+}]_i$ might originate from the mitochondria due to the generation of arachidonic acid. Arachidonic acid is also responsible for TG-induced neurite outgrowth. Prevention of a $[Ca^{2+}]_i$ increase by the use of the Ca^{2+} chelator, BAPTA, had no effect on TG-induced neurite outgrowth. Thus, TG-induced phospholipase A_2 activation is not dependent on a $[Ca^{2+}]_i$ increase and is attributable to depletion of intracellular Ca^{2+} stores. It has been shown previously that, in A-10 smooth muscle cells, depletion of Ca^{2+} pools, even in the absence of a $[Ca^{2+}]_i$ increase, is sufficient for the activation of phospholipase A_2 (Wolf et al., 1997). It is possible that both group IV and VI phospholipase A_2 are involved in TG-induced neurite outgrowth, because it is inhibited by both $AACOCF_3$ and HELSS. In addition, cytochrome P450 epoxygenase are also responsible for TG-induced neurite outgrowth in NG108-15 cells.

In NG108-15 cells, TG activated not only phospholipase A_2, but also sphingosine kinase, to generate arachidonic acid and S1P, respectively. Sphingolipid metabolites have recently been shown to act as a second messenger governing the fate of the cell. S1P, the product of sphingosine kinase, inhibits cell death, whereas ceramide, the product of sphingomyelinase, favors cell death. Thus, the relative levels of S1P and ceramide determine whether the cell will live or die (Cuvillier et al., 1996; Perry and Hannun, 1998; Pyne and Pyne, 2000). In addition, depletion of the intracellular nonmitochondrial Ca^{2+} stores by TG causes DDT_1MF-2 smooth muscle cells to enter a quiescent nonproliferative G_0-like phase, and arachidonic acid derivatives can mimic the effect of serum by inducing growth-arrested cells to re-enter the cell cycle (Graber et al., 1997). In human coronary artery vascular smooth muscle cells, the reduction in the activity and expression of phospholipase A_2 correlates with the reduction in proliferation with time in culture (Anderson et al., 1997). These studies collectively indicate that arachidonic acid plays an essential role in smooth muscle cell growth. In the current study, although caspase-3 was activated after 3 h of treatment with TG, cell death was not seen until 7 h. This delay in cell death might be explained by the TG-induced generation of S1P and arachidonic acid. However, our data further indicate that exogenous arachidonic acid does not prevent FCCP-induced cell death, whereas S1P does, and that inhibition of sphingosine kinase accelerates TG-induced cell death, thus ruling out a protective effect of arachidonic acid.

The NG108-15 cell line is a good model system for studying many aspects of neuronal differentiation and function. Treatment of these cells with dibutyryl cAMP induces morphological and biochemical changes that are characteristics of differentiated neuronal cells (Nirenberg et al., 1983). Previously, we have shown that, after treatment of NG108-15 cells with dibutyryl cAMP, the outgrowth of neurite-like processes and cell rounding coincide with increases in voltage-sensitive Ca^{2+} channel activity, Ca^{2+} accumulation in the intracellular Ca^{2+} stores, and the size of the IP_3- and GTP-releasable Ca^{2+} pools (Chueh et al., 1994). In the current study, nondifferentiated cells were used. Treatment of cells with TG induced the outgrowth of neurite-like processes and the cell bodies became rounded-up, characteristics of differentiated NG108-15 cells. However, these TG-induced morphological changes were not attributable to cAMP generation. It has been shown that exogenous S1P induces neurite retraction and cell rounding in N1E-115 neuroblastoma cells through a G protein-coupled receptor, because

microinjected S1P had no effect (Postma et al., 1996), and similar results have been obtained with PC12 cells (Sato et al., 1997; Van Brocklyn et al., 1999). In the current study, TG also stimulated S1P generation in NG108-15 cells, but outgrowth of neurite-like processes was induced. Because S1P can act as an extracellular agonist for cell surface receptors or an intracellular second messenger (Lee et al., 1998; Van Brocklyn et al., 1999; Pyne and Pyne, 2000), the functional role of S1P in mediating neurite outgrowth, either stimulation or inhibition, may depend on the mode of S1P generation.

Acknowledgments

We thank Dr. Thomas Barkas for helpful discussion.

References

Anderson KM, Roshak A, Winkler JD, McCord M, and Marshall LA (1997) Cytosolic 85-kDa phospholipase A_2-mediated release of arachidonic acid is critical for proliferation of vascular smooth muscle cells. *J Biol Chem* **272:**30504–30511.

Barnard EA (1996) The transmitter-gated channels: a range of receptor types and structures. *Trends Pharmacol Sci* **17:**305–309.

Berridge MJ (1998) Neuronal calcium signaling. *Neuron* **21:**13–26.

Bi Z and Reiss CS (1995) Inhibition of vesicular stomatitis virus infection by nitric oxide. *J Virol* **69:**2208–2213.

Carafoli E (1987) Intracellular calcium homeostasis. *Annu Rev Biochem* **56:**395–433.

Chen PF, Chin TY, and Chueh SH (1998) Ca^{2+} signaling induced by sphingosylphosphorylcholine and sphingosine 1-phosphate via distinct mechanisms in rat glomerular mesangial cells. *Kidney Int* **54:**1470–1483.

Chin TY and Chueh SH (1998) Sphingosylphosphorylcholine stimulates mitogen-activated protein kinase via a Ca^{2+}-dependent pathway. *Am J Physiol* **275:**C1255–C1263.

Choi DW (1988) Glutamate neurotoxicity and diseases of the nervous system. *Neuron* **1:**623–624.

Chueh SH and Kao LS (1994) Calcium signaling induced by bradykinin is synergistically enhanced by high K^+ in NG108-15 cells. *Am J Physiol* **266:**C1006–C1012.

Chueh SH, Kao LS, and Liu YT (1994) Enhanced calcium signaling events in neuroblastoma x glioma hybrid NG108-15 cells after treatment with dibutyryl cyclic AMP. *Brain Res* **660:**81–87.

Chueh SH, Song SL, and Liu TY (1995) Heterologous desensitization of opioid-stimulated Ca^{2+} increase by bradykinin or ATP in NG108-15 cells. *J Biol Chem* **270:**16630–16637.

Clapham DE (1995) Cell signaling. *Cell* **80:**259–268.

Cuvillier O, Pirianov G, Kleuser B, Vanek PG, Coso OA, Gutkind JS, and Spiegel S (1996) Suppression of ceramide-mediated programmed cell death by sphingosine-1-phosphate. *Nature (Lond)* **381:**800–803.

Denton RM and McCormack JG (1990) Ca^{2+} as second messenger within mitochondria of the heart and other tissues. *Annu Rev Physiol* **52:**451–466.

Edsall LC, Pirianov GG, and Spiegel S (1997) Involvement of sphingosine 1-phosphate in nerve growth factor-mediated neuronal survival and differentiation. *J Neurosci* **17:**6952–6960.

Gonzalez A, Schulz I, and Schmid A (2000) Agonist-evoked mitochondrial Ca^{2+} signals in mouse pancreatic acinar cells. *J Biol Chem* **275:**38680–38686.

Graber MN, Alfonso A, and Gill DL (1997) Recovery of Ca^{2+} pools and growth in Ca^{2+} pool-depleted cells is mediated by specific epoxyeicosatrienoic acids derived from arachidonic acid. *J Biol Chem* **272:**29546–29553.

Grynkiewicz G, Poenie M, and Tsien RY (1985) A new generation of Ca^{2+} indicators with greatly improved fluorescence properties. *J Biol Chem* **260:**3440–3450.

Gunter TE, Gunter KK, Sheu SS, and Gavin CE (1994) Mitochondrial calcium transport: physiological and pathological relevance. *Am J Physiol* **267:**C313–C339.

Hess P (1990) Calcium channels in vertebrate cells. *Annu Rev Neurosci* **13:**337–356.

Hsu LS, Chou WY, and Chueh SH (1995) Evidence for a Na^+/Ca^{2+} exchanger in neruoblastoma x glioma hybrid NG108-15 cells. *Biochem J* **309:**445–452.

Huang WC and Chueh SH (1996) Calcium mobilization from the intracellular mitochondrial and nonmitochondrial stores of the rat cerebellum. *Brain Res* **718:**151–158.

Ichas F and Mazat JP (1998) From calcium signaling to cell death: two conformations for the mitochondrial permeability transition pore. Switching from low- to high-conductance state. *Biochim Biophys Acta* **1366:**33–50.

Jones KH and Senft JA (1985) An improved method to determine cell viability by simultaneous staining with fluorescein diacetate-propidium iodide. *J Histochem Cytochem* **33:**77–79.

Lee MJ, Van Brocklyn JR, Thangada S, Liu CH, Hand AR, Menzeleev R, Spiegel S, and Hla T (1998) Sphingosine-1-phosphate as a ligand for the G protein-coupled receptor EDG-1. *Science (Wash DC)* **279:**1552–1555.

Nirenberg M, Wilson S, Higashida H, Rotter A, Kruegre K, Busis N, Ray R, Kenimer JG, and Adler M (1983) Modulation of synapse formation by cyclic adenosine monophosphate. *Science (Wash DC)* **222:**794–799.

Paschen W and Doutheil J (1999) Disturbances of the functioning of endoplasmic reticulum: a key mechanism underlying neuronal cell injury? *J Cereb Blood Flow Metabol* **19:**1–18.

Perry DK and Hannun YA (1998) The role of ceramide in cell signaling. *Biochim Biophys Acta* **1436:**233–243.

Philipson KD and Nicoll DA (1992) Sodium-calcium exchange. *Curr Opin Cell Biol* **4:**678–683.

Postma FR, Jalink K, Hengeveld T, and Moolenaar WH (1996) Sphingosine-1-phosphate rapidly induces rho-dependent neurite retraction: action through a specific cell surface receptor. *EMBO (Eur Mol Biol Organ) J* **15:**2388–2392.

Pyne S and Pyne NJ (2000) Sphingosine 1-phosphate signalling in mammalian cells. *Biochem J* **349:**385–402.

Sato K, Tomura H, Igarashi Y, Ui M, and Okajima F (1997) Exogenous sphingosine 1-phosphate induces neurite retraction possibly through a cell surface receptor in PC12 cells. *Biochem Biophys Res Commun* **240:**329–334.

Short AD, Bian J, Ghosh TK, Waldron RT, Rybak SL, and Gill DL (1993) Intracellular Ca^{2+} pool content is linked to control of cell growth. *Proc Natl Acad Sci USA* **90:**4986–4990.

Skryma R, Mariot P, Le Bourhis X, Van Coppenolle F, Shuba Y, Abeele FV, Legrand G, Humez S, Boilly B, and Prevarskaya N (2000) Store depletion and store-operated Ca^{2+} current in human prostate cancer LNCaP cells: involvement in apoptosis. *J Physiol* **527:**1.71–83.

Van Brocklyn JR, Tu Z, Edsall LC, Schmidt RR, and Spiegel S (1999) Sphingosine 1-phosphate-induced cell rounding and neurite retraction are mediated by the G protein-coupled receptor H218. *J Biol Chem* **274:**4626–4632.

Wertz IE and Dixit VM (2000) Characterization of calcium release-activated apoptosis of LNCaP prostate cancer cells. *J Biol Chem* **275:**11470–11477.

Wolf MJ, Wang J, Turk J, and Gross RW (1997) Depletion of intracellular calcium stores activates smooth muscle cell calcium-independent phospholipase A_2. *J Biol Chem* **272:**1522–1526.

Zhu X, Jiang M, Peyton M, Boulay G, Hurst R, Stefani E, and Birnbaumer L (1996) *trp*, a novel mammalian gene family essential for agonist-activated capacitative Ca^{2+} entry. *Cell* **85**:661–671.

Address correspondence to: Dr. Sheau-Huei Chueh, Department of Biochemistry, National Defense Medical Center 161, Section 6, Min-Chuan East Road, Taipei, Taiwan, Republic of China. E-mail: shch@ndmctsgh.edu.tw